

# Direct Comparison of Chiral Substituent Effects for Viologens in Stereoselective Photoinduced Electron-Transfer Reactions with Zinc Myoglobin

Hiroshi Takashima,<sup>\*1</sup> Satomi Shibata,<sup>1</sup> Yuka Sekiguchi,<sup>1</sup> Yoshitane Imai,<sup>2</sup> and Keiichi Tsukahara<sup>\*1</sup>

<sup>1</sup>Department of Chemistry, Faculty of Science, Nara Women's University, Nara 630-8506

<sup>2</sup>Department of Applied Chemistry, Faculty of Science and Engineering, Kinki University, Higashi-Osaka 577-8502

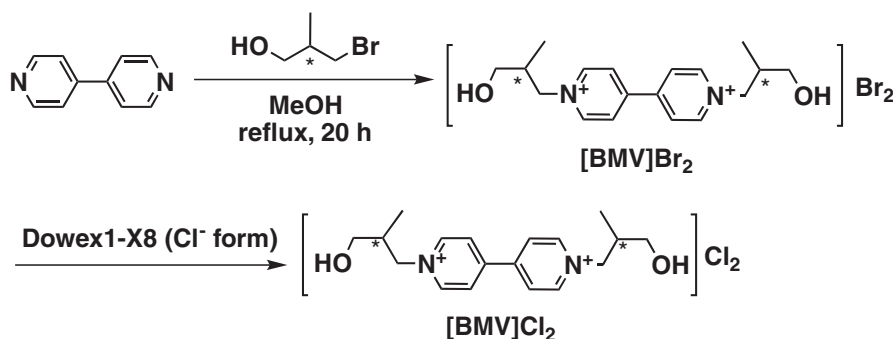
Received April 7, 2009; E-mail: hiroshi@cc.nara-wu.ac.jp, tsukahara@cc.nara-wu.ac.jp

In order to understand the detailed mechanisms of stereoselective photoinduced electron-transfer (ET) reactions of zinc-substituted myoglobin (ZnMb) with optically active viologens by flash photolysis, we prepared new optically active agents, such as (*R,R*)- and (*S,S*)-1,1'-bis(3-hydroxy-2-methylpropyl)-4,4'-bipyridinediylum dichloride ([BMV]Cl<sub>2</sub>). The photo-excited triplet state of ZnMb, <sup>3</sup>(ZnMb)\*, was successfully quenched by (*R,R*)- and (*S,S*)-[BMV]<sup>2+</sup> ions to form the radical pair of ZnMb cation (ZnMb<sup>•+</sup>) and (*R,R*)- and (*S,S*)-[BMV]<sup>•+</sup>, followed by a thermal back ET reaction to the ground state. The ratio of the rate constants (*k<sub>q</sub>*) for ET quenching at 25 °C, *k<sub>q</sub>*(*R,R*)/*k<sub>q</sub>*(*S,S*) = 1.1, indicates that the (*R,R*)-[BMV]<sup>2+</sup> preferentially quenches <sup>3</sup>(ZnMb)\*. The selectivity of the rate constants (*k<sub>b</sub>*) for the back ET from (*R,R*)- and (*S,S*)-[BMV]<sup>•+</sup> to ZnMb<sup>•+</sup> at 25 °C was *k<sub>b</sub>*(*R,R*)/*k<sub>b</sub>*(*S,S*) = 0.83. The highest stereoselectivity of 1.3 for [BMV]<sup>•+</sup> was found at low temperature (10 °C) in the thermal back ET reaction, where  $\Delta\Delta H^\ddagger(\text{R-S}) = 6.2 \pm 1.9 \text{ kJ mol}^{-1}$  and  $\Delta\Delta S^\ddagger(\text{R-S}) = 19 \pm 2 \text{ J mol}^{-1} \text{ K}^{-1}$  were obtained. The structural differences between [BMV]<sup>2+</sup> and the other viologens imply that the bulky aromatic substituent seems to be more important than the distance from the chiral center to the viologen moiety in order to enhance the ET stereoselectivity.

Photoinduced electron-transfer (ET) reactions between hemoproteins and small molecules, to transport electrons initiated by light energy, have received considerable attention in the field of bioinorganic chemistry.<sup>1–8</sup> Much effort on bimolecular photoinduced ET reactions using zinc-hemoprotein has been carried out, because its photoexcited triplet state can act as a strong reductant having a lifetime of several milliseconds.<sup>9–13</sup> Several reaction mechanisms, including conformational gating,<sup>14</sup> have been suggested for zinc-cytochrome *c*,<sup>15</sup> –hemoglobin,<sup>16,17</sup> and –myoglobin (ZnMb).<sup>3,5,18–20</sup> As the charge, the conformation, the steric bulk, and other factors of the external quenchers may affect the ET reactions, a series of organic quenchers, such as methyl viologen<sup>18,19,21,22</sup> and quinones,<sup>23</sup> have been utilized so far. Along this line, since an obvious property of the protein surface is chirality, stereoselective bimolecular photoinduced ET with a hemoprotein has become a recent research topics. After the first demonstration of the stereoselectivity of outer-sphere ET reactions of metal complexes,<sup>24</sup> the following two main questions concerning stereoselective ET reactions by optically active compounds should be considered. (1) How does chiral substitution of small molecules affect the stereoselectivity of ET? and (2) How is the chiral environment around the reactive site at the surface of hemoprotein recognized? Even partially successful ET systems should help to answer these questions, for example, the stereoselective ET reaction of chiral metal complexes with spinach plastocyanin,<sup>25,26</sup> horse cytochrome *c*,<sup>27,28</sup> and plant ferredoxin.<sup>29</sup> Nevertheless, no experiments of the stereoselectivity of photoinduced ET reactions between metalloprotein and a chiral organic agent

have been conducted so far, except for our viologen and quinolinium ion systems.<sup>30–33</sup> One of the reasons is the lack of systematic study utilizing synthetic chiral molecules.

We have reported the synthesis and photophysical properties of a variety of chemically modified viologens and bisviologens. Some of them are appended optically active *N*-[1-(1-naphthyl), 1-phenyl, and 1-cyclohexylethyl]carbamoymethyl groups ([NOAV]<sup>2+</sup>, [OAV]<sup>2+</sup>, and [CHOAV]<sup>2+</sup>, respectively).<sup>34,35</sup> They certainly acted as good electron acceptors for the excited triplet state of ZnMb, <sup>3</sup>(ZnMb)\*, and demonstrated stereoselective ET reactions.<sup>30</sup> Their stereoselectivities evaluated from the ET rate constants, however, are relatively small and this result makes slightly difficult discussion of the detailed mechanism of the stereoselectivity achieved in bimolecular ET reactions. The small selectivity in these systems may arise because the reactive center in viologens is far from the chiral recognition centers. Therefore, further extensive design of new optically active viologen derivatives should be needed to construct more apparent stereoselective ET systems. In this manuscript, we newly describe the convenient synthesis of a viologen derivative with chiral centers near the reactive center, [BMV]<sup>2+</sup>, as shown in Scheme 1. This undergoes effective one-electron redox reactions with photo-generated <sup>3</sup>(ZnMb)\* and temperature-dependent kinetic studies performed by flash photolysis are presented. By comparing the structural features of [BMV]<sup>2+</sup> with the other viologens, we discuss how the bulky aromatic substituent and the distance from the chiral center to the viologen moiety are important for stereoselective photoinduced ET reactions with ZnMb.

Scheme 1. Synthesis of [BMV]Cl<sub>2</sub>.

### Experimental

**Materials.** Metmyoglobin from horse heart muscle (Sigma) was purified as previously described.<sup>36</sup> The reconstitution of apomyoglobin with protoporphyrinIXato(2-)-zinc(II) (Sigma) was carried out at 4 °C in the dark using a method previously published and the concentrations of ZnMb were spectrophotometrically determined ( $\epsilon_{428} = 1.53 \times 10^5 \text{ M}^{-1} \text{ cm}^{-1}$ ).<sup>37,38</sup> The ZnMb solution, whose absorption ratio  $A_{428}/A_{280}$  was greater than 9.5, was used for kinetic measurements. (*R,R*)- and (*S,S*)-1,1'-Bis(2-methyl-3-hydroxypropyl)-4,4'-bipyridinium salts were prepared from 4,4'-bipyridine (Tokyo Kasei Kogyo Co., Ltd.). (*R*)- or (*S*)-3-Bromo-2-methyl-1-propanol was purchased from Sigma-Aldrich Co., Ltd. and used without further purification. The ion exchange resin, Dowex1-X8 (Cl<sup>-</sup> form), was obtained from the Dow Chemical Co. All other reagents and solvents were of reagent grade. All of the aqueous solutions were prepared from redistilled water. The ionic strength (*I*) of the solutions was adjusted with NaCl.

**Preparation of (*R,R*)- or (*S,S*)-1,1'-Bis(3-hydroxy-2-methyl-propyl)-4,4'-bipyridinediylum Dichloride [(*R,R*)-[BMV]Cl<sub>2</sub> or (*S,S*)-[BMV]Cl<sub>2</sub>].** A 20 mL three-neck round-bottomed flask equipped with a condenser and a magnetic stirring bar was charged with 4,4'-bipyridine (0.10 g, 0.64 mmol), (*R*)- or (*S*)-3-bromo-2-methyl-1-propanol (0.24 g, 1.6 mmol) and anhydrous acetonitrile (4.0 mL). Under argon atmosphere, the resulting solution was heated to reflux for 20 h. After cooling down to room temperature, the solvent was removed on a rotary evaporator. The residue was washed with diethyl ether and dichloromethane in a Buechner funnel to remove excess of 3-bromo-2-methyl-1-propanol. The resulting residue was recrystallized from ethanol solution and lightly yellow solid was collected. Yield 0.21–0.24 g (72–81%). To conduct the kinetic measurements in an aqueous solution, the counter anions of [BMV]Br<sub>2</sub> were converted to the Cl<sup>-</sup> form. The [BMV]Br<sub>2</sub> was dissolved in 10 mL of MeOH and column chromatography on Dowex1-X8 (Cl<sup>-</sup> form,  $\phi 2.5 \times 20 \text{ cm}$ , MeOH) afforded [BMV]Cl<sub>2</sub>. <sup>1</sup>H NMR (300 MHz, DMSO-*d*<sub>6</sub>, 298 K):  $\delta$  0.88 (d, 6H, *J* = 6.9 Hz), 2.31 (m, 2H), 3.49 (m, 4H), 4.58 (m, 2H), 4.71 (m, 2H), 8.79 (d, 4H, *J* = 7.1 Hz), 9.35 (d, 4H, *J* = 7.1 Hz). UV (0.010 M phosphate buffer at pH 7.0,  $\lambda_{\text{nm}}$  ( $\epsilon/10^4 \text{ M}^{-1} \text{ cm}^{-1}$ )): 264 (2.45). Anal. Calcd for C<sub>18</sub>H<sub>26</sub>N<sub>2</sub>O<sub>2</sub>·Cl<sub>2</sub> (MW: 373.32): C, 57.91; H, 7.02; N, 7.50%. Found: C, 57.48; H, 6.64; N, 7.00%.

**Kinetic Measurements.** The procedure for the kinetic studies was the same as that previously reported.<sup>30</sup> Sample solutions were gently purged with Ar gas and then carefully degassed by freeze-pump-thaw cycles. The ratio of  $A_{428}/A_{280}$  was checked for each solution. Single flash-photolysis experiments were done in deaerated solutions containing ZnMb ( $3.0 \times 10^{-6} \text{ M}$ ) and quench-

ers ( $0\text{--}2.5 \times 10^{-5} \text{ M}$ ) at various temperatures (10–30 °C), pH 7.0 (0.010 M phosphate buffer), and *I* = 0.020 M using a Photol RA-412 pulse flash apparatus with a 30  $\mu\text{s}$  pulse-width Xe lamp ( $\lambda > 450 \text{ nm}$ ; a Toshiba Y-47 glass filter). The spectral absorption changes during the reaction were monitored at 460 nm for the decay of <sup>3</sup>(ZnMb)\*, and at 680 nm for the formation and decay of the radical cation ZnMb<sup>•+</sup>.

**Other Measurements.** The UV-vis and CD spectra were measured with Shimadzu UV-2550 and JASCO J720 instruments, respectively. The <sup>1</sup>H NMR spectra were recorded at 298 K with a Varian Mercury M300 Spectrometer (300 MHz) in DMSO-*d*<sub>6</sub> using tetramethylsilane as an internal standard. Cyclic voltammetry was done in N<sub>2</sub>-saturated 0.050 M KCl aqueous solutions by using an ALS Electrochemical Analyzer Model 610B instrument. A three-electrode system (BAS Inc.) was used with a Pt auxiliary electrode and a Pt working electrode against an Ag/AgCl (3.33 M KCl in water) reference electrode. The potentials were calibrated by using 1,1'-dimethyl-4,4'-bipyridinediylum dichloride, [MV]Cl<sub>2</sub> ( $E^0 = -0.45 \text{ V}$  vs. NHE (normal hydrogen electrode)). The pHs of the solutions were measured using a Hitachi-Horiba F-14RS pH meter.

### Results and Discussion

**Synthesis and Redox Properties of [BMV]<sup>2+</sup>.** The syntheses of the (*R,R*)- and (*S,S*)-1,1'-bis(3-hydroxy-2-methyl-propyl)-4,4'-bipyridinediylum dichloride were conducted using 4,4'-bipyridine and (*R*)- and (*S*)-3-bromo-2-methyl-1-propanol as materials, respectively (Scheme 1). After recrystallization from ethanol, the bromide salts of (*R,R*)- and (*S,S*)-[BMV]Br<sub>2</sub> were obtained in good yields. The bromide form of [BMV]Br<sub>2</sub> was then converted to the chloride form by an ion-exchange Dowex1-X8 resin in MeOH. These were satisfactorily identified by <sup>1</sup>H NMR, UV, and CD spectroscopies and elemental analysis (see Experimental).

The UV spectrum of [BMV]Cl<sub>2</sub> in a 0.010 M phosphate buffer (pH 7.0) showed a sharp band at 264 nm ( $\epsilon = 2.45 \times 10^4 \text{ M}^{-1} \text{ cm}^{-1}$ ). The CD spectra were recorded with a 1 cm cell cuvette at 25 °C in a 0.010 M phosphate buffer (pH 7.0) to examine the optical purity of both isomers. The positive sign at 220–270 nm and the negative sign at 200–220 and 270–290 nm regions appeared for (*R,R*)-[BMV]<sup>2+</sup>, whereas the negative sign at 220–270 nm and the positive sign at 200–220 and 270–290 nm regions were obtained for (*S,S*)-[BMV]<sup>2+</sup> (Figure S1 in Supporting Information). The peak intensities of positive and negative peaks for both isomers were nearly the same, for example,  $\Delta\epsilon_{253} = +0.81 \pm 0.05 \text{ M}^{-1} \text{ cm}^{-1}$  for the *R,R* isomer and  $-0.82 \pm 0.05 \text{ M}^{-1} \text{ cm}^{-1}$  for the *S,S* isomer. These results

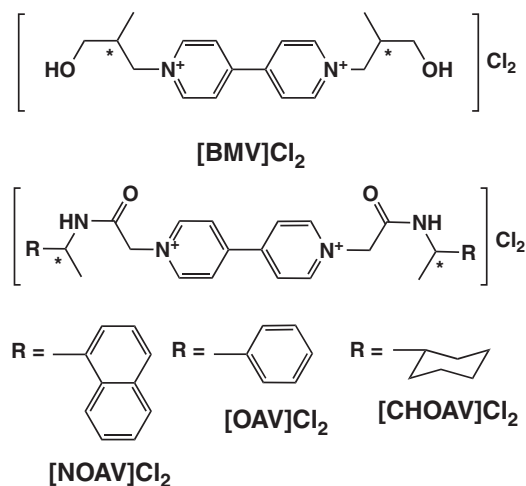


Chart 1.

clearly indicate that the absolute configurations have always been preserved from any racemizations during the synthesis.

Next, in order to evaluate the redox properties of [BMV]Br<sub>2</sub>, cyclic voltammograms were recorded in 0.050 M KCl aqueous solutions at 25 °C under a N<sub>2</sub> atmosphere with a Pt electrode used as the working electrode. It is well known that methyl viologen, [MV]Cl<sub>2</sub>, has one-electron redox potentials at −0.45 and −0.88 V (vs. NHE) in water.<sup>32,39</sup> For the optically active (*R,R*)-[BMV]Br<sub>2</sub> and (*S,S*)-[BMV]Br<sub>2</sub>, the quasi-reversible one-electron redox waves were both presented at −0.41 V (vs. NHE) in an aqueous solution ([BMV]<sup>2+</sup>/[BMV]<sup>•+</sup>); See Figure S2 in Supporting Information) calibrated by using [MV]Cl<sub>2</sub>. We noted that a similar electrochemical behavior, such as the quasi-reversible one-electron redox wave at −0.41 V ([BMV]<sup>2+</sup>/[BMV]<sup>•+</sup>), was observed using the Cl<sup>−</sup> forms of (*R,R*)-[BMV]<sup>2+</sup> and (*S,S*)-[BMV]<sup>2+</sup>. Based on these measurements, the new optically active viologen, [BMV]<sup>2+</sup>, can be expected to perform as a good electron acceptor for the excited triplet state of ZnMb similar to the [NOAV]<sup>2+</sup>, [OAV]<sup>2+</sup>, and [CHOAV]<sup>2+</sup> as listed in Chart 1.<sup>30</sup>

Viologens are easily reduced by dithionite ions in an aqueous solution under an Ar atmosphere to give radical cations.<sup>39–42</sup> We also observed the absorption spectrum of the radical cation of [BMV]<sup>•+</sup> (4.0 × 10<sup>−5</sup> M) in the presence of a slight excess of dithionite ion. Figure S3 in Supporting Information showed a sharp (λ<sub>max</sub> = 397 nm) and a broad (λ<sub>max</sub> = 600 nm) peaks, indicating [BMV]<sup>•+</sup> is presented as a monomer form at pH 7.0 in a 0.010 M phosphate buffer.<sup>34</sup>

**Photoinduced ET Reaction of ZnMb.** The photo-excited <sup>3</sup>(ZnMb)\* is generally known to be quenched by several electron acceptors, whereas the excited singlet state, <sup>1</sup>(ZnMb)\*, is not quenched.<sup>5</sup> Such quenching has been discussed as an intermolecular ET mechanism. Figure 1a displays the first-order decay of the transient absorption of <sup>3</sup>(ZnMb)\* monitored at 460 nm in the presence of [BMV]<sup>2+</sup> at 25 °C, pH 7.0 (0.010 M phosphate buffer), and *I* = 0.020 M. The rate constant for the quenching reaction of <sup>3</sup>(ZnMb)\*, *k*<sub>obsd</sub>, linearly increased with the increasing concentration of [BMV]<sup>2+</sup> at various temperatures (Figure 2), indicating that no appreciable complex was formed between <sup>3</sup>(ZnMb)\* and [BMV]<sup>2+</sup>. We also

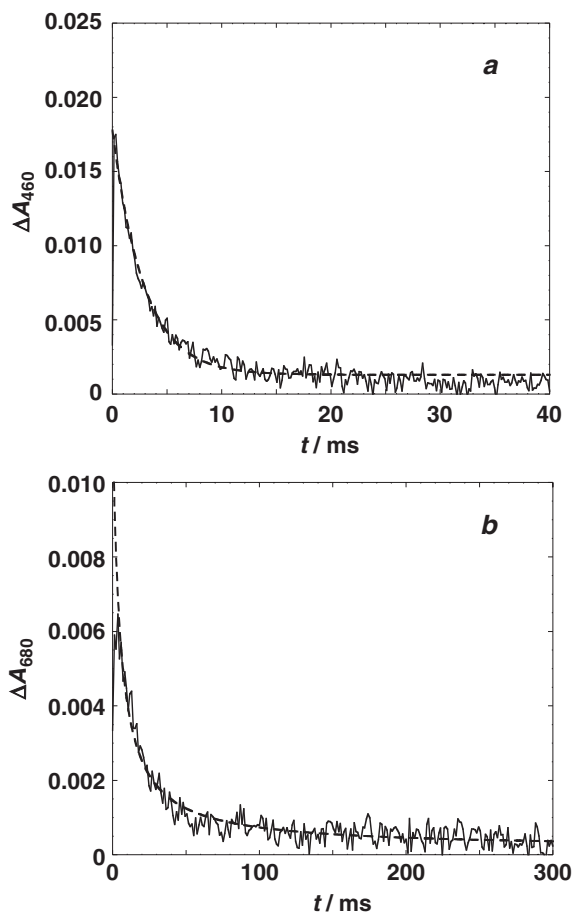


**Figure 1.** Absorbance changes after irradiation of ZnMb (3.0 × 10<sup>−6</sup> M) with a Xe flash lamp in the presence of (*R,R*)-[BMV]<sup>2+</sup> (1.7 × 10<sup>−5</sup> M) at 25 °C, pH 7.0 (0.010 M phosphate buffer), and *I* = 0.020 M. (a) Decay of <sup>3</sup>(ZnMb)\* at 460 nm. The broken line is fitted to the first-order decay kinetics. (b) Decay of ZnMb<sup>•+</sup> at 680 nm. The broken line is fitted to eq 1.

monitored the kinetic trace at 680 nm for the formation and decay of the radical cation of ZnMb<sup>•+</sup>.<sup>30,43</sup> The transient absorption kinetics of the thermal back ET in Figure 1b obeyed a second-order rate law, suggesting that an equimolar amount of ZnMb<sup>•+</sup> with a [BMV]<sup>•+</sup> radical cation formed.

The photoinduced ET reaction of ZnMb with [BMV]<sup>2+</sup> is represented in Scheme 2. The quenching rate constant (*k*<sub>q</sub>) was thus obtained from the slope of the plots of *k*<sub>obsd</sub> versus the concentration of [BMV]<sup>2+</sup>. As the thermal ET reaction to the ground state was much slower than the quenching reaction (Figure 1b) and the quantum yield of the quenching ET reaction would be nearly unity (see next section), the second-order rate constant of the thermal ET reaction (*k*<sub>b</sub>) was evaluated during the latter portion of the decay of ZnMb<sup>•+</sup> at 680 nm, which overlaps with the partial absorption of [BMV]<sup>•+</sup>, after the quenching of <sup>3</sup>(ZnMb)\* was completed (eq 1):

$$A_t = (A_0 + k_b[A]_0 A_\infty t) / (1 + k_b[A]_0 t) \quad (1)$$

Here *A*<sub>0</sub>, *A*<sub>*t*</sub>, and *A*<sub>∞</sub> are the absorbances at time 0, *t*, and infinity, respectively, and [*A*]<sub>0</sub> is the initial concentration of

$\text{ZnMb}^{\bullet+}$ . Three unknown parameters,  $A_0$ ,  $k[A]_0$ , and  $A_\infty$  were simultaneously estimated. The value of  $k_b$  was then determined using the value of  $[A]_0$  calculated from the concentration of  $^3(\text{ZnMb})^*$  ( $\Delta\epsilon_{428} = \epsilon(\text{ground}) - \epsilon(\text{triplet}) = 1.00 \times 10^5 \text{ M}^{-1} \text{ cm}^{-1}$ ).<sup>9</sup>

**Stereoselective ET Quenching Reactions at 25 °C.** The ET quenching reaction of  $^3(\text{ZnMb})^*$  by  $[\text{BMV}]^{2+}$  is exothermic,  $\Delta G^0 = -0.39 \text{ eV}$ , based on the redox potentials. Under the present experimental conditions, in which the  $[\text{BMV}]^{2+}$  ion

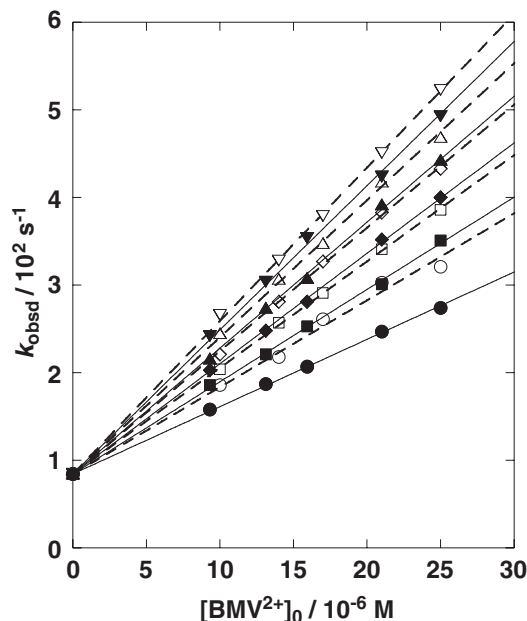
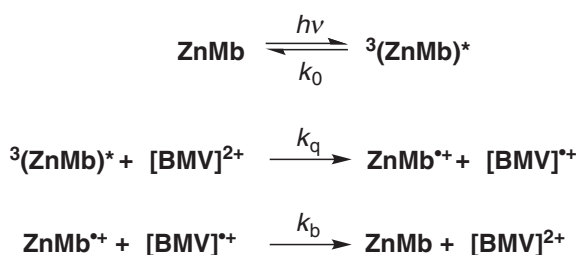


**Figure 2.** Plots of  $k_{\text{obsd}}$  versus  $[\text{BMV}^{2+}]_0$  for the quenching of  $^3(\text{ZnMb})^*$  by  $(R,R)$ - $[\text{BMV}]^{2+}$  (open symbols) and  $(S,S)$ - $[\text{BMV}]^{2+}$  (closed symbols) at pH 7.0 (0.010 M phosphate buffer) and  $I = 0.020 \text{ M}$ : (circles) 10 °C; (squares) 15 °C; (diamonds) 20 °C; (up triangles) 25 °C; (down triangles) 30 °C.



**Scheme 2.** Photoinduced ET reaction between ZnMb and  $[\text{BMV}]^{2+}$ .

is used in large excess over  $^3(\text{ZnMb})^*$ , with concentration ( $[^3(\text{ZnMb})^*]_0$ ) of  $1.8 \times 10^{-6} \text{ M}$ , the electron-transfer quenching was almost complete: >98% for  $[\text{BMV}]^{2+}$ . The rate constants ( $k_q$ ) for the ET quenching reactions of  $(R,R)$ - $[\text{BMV}]^{2+}$  and  $(S,S)$ - $[\text{BMV}]^{2+}$  at 25 °C were determined as  $k_q(R,R) = (1.6 \pm 0.1) \times 10^7 \text{ M}^{-1} \text{ s}^{-1}$  and  $k_q(S,S) = (1.4 \pm 0.2) \times 10^7 \text{ M}^{-1} \text{ s}^{-1}$  (Table 1). During the quenching reaction of  $(R,R)$ - $[\text{BMV}]^{2+}$  and  $(S,S)$ - $[\text{BMV}]^{2+}$ , the ratio of the rate constants was found to be  $k_q(R,R)/k_q(S,S) = 1.1$  at 25 °C.

In the case of chiral viologens, we have proposed that the bimolecular quenching reactions were controlled by the conformational gating of ZnMb,<sup>14,17,18,44</sup> according to the driving force dependence of the ET rate constants. In order to evaluate the present quenching mechanism between  $^3(\text{ZnMb})^*$  and  $[\text{BMV}]^{2+}$ , we calculated the rate constants using the following Marcus theory (eq 2).<sup>45,46</sup>

$$k_{12} = (k_{11}k_{22}f_{12}K_{12})^{1/2} \quad (2)$$

where,  $k_{12}$  is the rate constant for the cross reaction,  $k_{11}$  and  $k_{22}$  are those for the self-exchange reactions of the donor and acceptor, respectively,  $K_{12}$  is the equilibrium constant for the cross reaction, and  $f_{12}$  is given by

$$\ln f_{12} = (\ln K_{12})^2 / 4 \ln(k_{11}k_{22}/10^{22}) \quad (3)$$

Equations 2 and 3 are also represented by

$$\ln k_{12} = 25.3 - (\lambda_{12} + \Delta G^0)^2 / 4\lambda_{12}RT \quad (4)$$

where  $\lambda_{12}$  is the reorganization energy for the reaction, and equals the average of those of the donor and acceptor,  $(\lambda_{11} + \lambda_{22})/2$ . By using the data  $k_{11} = 2.6 \times 10^5 \text{ M}^{-1} \text{ s}^{-1}$  for  $\text{ZnMb}^{\bullet+}/^3(\text{ZnMb})^*$  ( $\lambda_{11} = 1.32 \text{ eV}$ ),<sup>47</sup>  $k_{22} = 1.0 \times 10^8 \text{ M}^{-1} \text{ s}^{-1}$  for  $[\text{BMV}]^{2+}/[\text{BMV}]^{\bullet+}$  couple ( $\lambda_{22} = 0.71 \text{ eV}$ ),<sup>31</sup> and  $K_{12} = 3.8 \times 10^6$  for  $[\text{BMV}]^{2+}$  (the redox potential of  $\text{ZnMb}^{\bullet+}/^3(\text{ZnMb})^*$  is  $-0.80 \text{ V}$  and  $\Delta G^0 = -0.39 \text{ eV}$ ),<sup>48</sup> the calculated rate constants,  $k_{12}$ , is  $2.3 \times 10^9 \text{ M}^{-1} \text{ s}^{-1}$  ( $f_{12} = 5.5 \times 10^{-2}$ ) for  $[\text{BMV}]^{2+}$  at 25 °C. The observed ET rate constant is not close to the calculated one. It is noteworthy that the ET reactions between  $^3(\text{ZnMb})^*$  and chiral quinolinium ions and cinchona alkaloid derivatives are controlled by the ET step, and the driving-force dependent ET reactions, whose rate constants are calculated by using the value of  $k_{11}$  and  $\lambda_{11}$  for  $\text{ZnMb}^{\bullet+}/^3(\text{ZnMb})^*$  as described above, are apparently observed.<sup>29,31</sup> However, in some cases of bimolecular quenching between  $^3(\text{ZnMb})^*$  and other quenchers, such as anthraquinone-2-sulfonate, methyl viologen, and dioxygen, Barboy and Feitelson have proposed a conformational gating mechanism.<sup>18,19</sup> We have supported the mechanism controlled by conformational change of ZnMb for the quenching reactions with

**Table 1.** Rate Constants Determined for the ET Reactions between ZnMb and Optically Active  $(R,R)$ - and  $(S,S)$ - $[\text{BMV}]^{2+}$  Ions at pH 7.0 and  $I = 0.020 \text{ M}$

Temperature/°C	$k_q/10^7 \text{ M}^{-1} \text{ s}^{-1}$		Selectivity	$k_b/10^8 \text{ M}^{-1} \text{ s}^{-1}$		Selectivity
	$(R,R)$ - $[\text{BMV}]^{2+}$	$(S,S)$ - $[\text{BMV}]^{2+}$		$(R,R)$ - $[\text{BMV}]^{\bullet+}$	$(S,S)$ - $[\text{BMV}]^{\bullet+}$	
10	$0.99 \pm 0.05$	$0.77 \pm 0.04$	$1.3 \pm 0.1$	$0.57 \pm 0.03$	$0.75 \pm 0.04$	$0.76 \pm 0.08$
15	$1.2 \pm 0.1$	$1.1 \pm 0.1$	$1.2 \pm 0.1$	$0.71 \pm 0.04$	$0.90 \pm 0.05$	$0.79 \pm 0.08$
20	$1.4 \pm 0.1$	$1.3 \pm 0.1$	$1.1 \pm 0.1$	$0.93 \pm 0.05$	$1.1 \pm 0.1$	$0.85 \pm 0.08$
25	$1.6 \pm 0.1$	$1.4 \pm 0.2$	$1.1 \pm 0.1$	$1.0 \pm 0.1$	$1.2 \pm 0.1$	$0.83 \pm 0.08$
30	$1.8 \pm 0.1$	$1.7 \pm 0.2$	$1.1 \pm 0.1$	$1.3 \pm 0.1$	$1.4 \pm 0.1$	$0.93 \pm 0.08$

chiral viologen derivatives.<sup>3,30,31,37,44,49</sup> Thus, we assume that the present quenching of  $^3(\text{ZnMb})^*$  by  $[\text{BMV}]^{2+}$  is controlled by conformational change of ZnMb, not by the ET step.

The quenching reactions of  $^3(\text{ZnMb})^*$  by several reactants have been discussed in terms of two mechanisms: (i) The reactant loosely associates or only collides with the ZnMb surface. (ii) The reactant diffuses through the protein and the diffusion is gated.<sup>30</sup> However, large quenchers of viologens may not diffuse into the heme pocket and the reaction might occur at the surface of the protein. This has been also confirmed by a time-resolved FT-EPR study.<sup>23</sup> Figure 3 illustrates one of the plausible structures of the ZnMb/ $[\text{BMV}]^{2+}$  complex. A comparison of the actual size of  $[\text{BMV}]^{2+}$  with that of ZnMb indicates that the  $[\text{BMV}]^{2+}$  ion can cover the heme pocket when it attacks the ZnMb surface. Although the Mb surface is cationic at neutral pH, the cationic  $[\text{BMV}]^{2+}$  loosely associates with the amino acid residues at the surface of ZnMb, thereby inducing a conformational change of  $^3(\text{ZnMb})^*$  to an active form.

We have also reported the stereoselective thermal electron-transfer reactions between met-myoglobin and optically active viologen radicals,  $[\text{OAV}]^{\bullet+}$  and  $[\text{CHOAV}]^{\bullet+}$ .<sup>35</sup> In such a system, metMb moderately interacted with the viologen-radical cation to form a complex, followed by an intramolecular ET reaction. The calculated intramolecular ET rate constant and the association constant indicate that there is stereoselectivity in both the chiral association and intramolecular ET processes. Although both of these constants could not be clarified for the present  $^3(\text{ZnMb})^* - [\text{BMV}]^{2+}$  system under our experimental conditions, they may also be important for explaining the

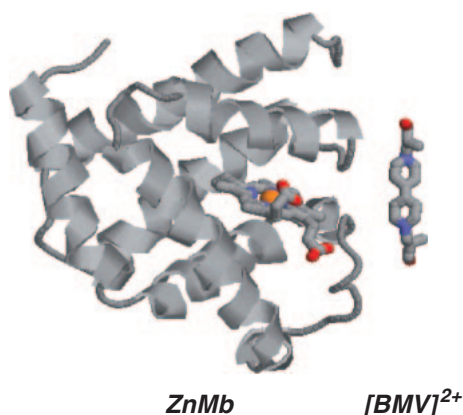


**Figure 3.** Illustration of the plausible structure of a ZnMb/ $(R,R)$ - $[\text{BMV}]^{2+}$  complex by a RasMol software. A favorable orientation of  $[\text{BMV}]^{2+}$  for access to the ZnMb surface is presented.

difference in the ET rate caused by the chirality. We herein note that previous results for the quenching reaction of  $^3(\text{ZnMb})^*$  by the optically active viologens,  $[\text{NOAV}]^{2+}$ ,  $[\text{OAV}]^{2+}$ , and  $[\text{CHOAV}]^{2+}$  (Chart 1), are summarized in Table 2 and the quenching rate constants ( $k_q$ ) for these systems were somewhat higher than that for  $[\text{BMV}]^{2+}$  and larger stereoselectivities were also observed. The structural features of the chiral substituents on the viologen center can directly reflect on the ET stereoselectivities. Two chiral centers are appended via a methylene group to yield  $[\text{BMV}]^{2+}$ , whereas the longer amide spacer is utilized to connect for the previously designed viologens,  $[\text{NOAV}]^{2+}$ ,  $[\text{OAV}]^{2+}$ , and  $[\text{CHOAV}]^{2+}$ . We have previously suggested that the hydrogen bonding of the amide group of the chiral viologen with the side chain of the polypeptide of Mb plays an important role in the binding and stereoselectivity.<sup>35</sup> Therefore, both the structural bulkiness, such as phenyl and naphthyl groups, and the hydrogen bonding of the spacer are important to provide a higher stereoselectivity in the bimolecular ET reactions with Mb. In the present ZnMb- $[\text{BMV}]^{2+}$  system, two chiral centers can be appropriately recognized by the chiral surface of ZnMb, but the conformational difference between S,S and R,R isomers is small and could not lead to large stereoselectivities in quenching.

#### Stereoselectivity in Thermal ET to the Ground State.

The thermal back ET reaction between  $\text{ZnMb}^{\bullet+}$  and the chiral viologen radical cation,  $[\text{BMV}]^{\bullet+}$ , has a stereoselectivity for (S,S)- $[\text{BMV}]^{\bullet+}$ . The second-order rate constants ( $k_b$ ) for the thermal back ET at 25 °C are shown in Table 1 and were determined to be  $k_b(R,R) = (1.0 \pm 0.1) \times 10^8 \text{ M}^{-1} \text{ s}^{-1}$  and  $k_b(S,S) = (1.2 \pm 0.1) \times 10^8 \text{ M}^{-1} \text{ s}^{-1}$ . In this study, we similarly obtained the calculated rate constant for the thermal back ET reaction,  $k_{12} = 2.6 \times 10^{10} \text{ M}^{-1} \text{ s}^{-1}$  ( $f_{12} = 7.2 \times 10^{-17}$ ) for  $[\text{BMV}]^{\bullet+}$  at 25 °C using the data  $k_{11} = 2.6 \times 10^5 \text{ M}^{-1} \text{ s}^{-1}$  for  $\text{ZnMb}^{\bullet+}/\text{ZnMb}$  ( $\lambda_{11} = 1.32 \text{ eV}$ ), and  $K_{12} = 3.5 \times 10^{23}$  for  $[\text{BMV}]^{\bullet+}$  ( $\Delta G^0 = -1.39 \text{ eV}$ ). This is also different from that of the observed value (Table 1), indicating that the thermal back ET reaction is similarly controlled by the conformational change of  $\text{ZnMb}^{\bullet+}$ . The back ET selectivity for  $[\text{BMV}]^{\bullet+}$  at 25 °C was found to be  $k_b(S,S)/k_b(R,R) = 1.2$  (Table 2) and the highest stereoselectivity of 1.3 was observed at low temperature (10 °C). Since the one-electron reduced radical,  $[\text{BMV}]^{\bullet+}$ , generated from the quenching of the photoexcited  $^3(\text{ZnMb})^*$  are less positive, we suggest that the charge effect on the viologen moiety is as important as the conformational effect to explain such a temperature-dependent selectivity in the thermal back ET. In the following section, a further discussion based on the activation parameters will be described to clarify the mechanisms.

**Table 2.** Rate Constants Determined for the ET Reactions between ZnMb and Optically Active Several Quenchers at 25 °C, pH 7.0 (0.010 M Phosphate Buffer), and  $I = 0.020 \text{ M}$

Quencher	$k_q/10^7 \text{ M}^{-1} \text{ s}^{-1}$		Selectivity	$k_b/10^8 \text{ M}^{-1} \text{ s}^{-1}$		Selectivity
	S,S isomer	R,R isomer		S,S isomer	R,R isomer	
$[\text{NOAV}]^{2+a)}$	$7.1 \pm 0.2$	$4.8 \pm 0.2$	$1.5 \pm 0.1$	$2.5 \pm 0.1$	$1.7 \pm 0.1$	$1.4 \pm 0.1$
$[\text{OAV}]^{2+a)}$	$3.9 \pm 0.1$	$2.9 \pm 0.1$	$1.3 \pm 0.1$	$1.4 \pm 0.1$	$0.98 \pm 0.08$	$1.4 \pm 0.1$
$[\text{CHOAV}]^{2+a)}$	$4.2 \pm 0.1$	$3.4 \pm 0.1$	$1.2 \pm 0.1$	$1.8 \pm 0.2$	$1.4 \pm 0.1$	$1.3 \pm 0.1$
$[\text{BMV}]^{2+b)}$	$1.4 \pm 0.2$	$1.6 \pm 0.1$	$0.88 \pm 0.08$	$1.2 \pm 0.1$	$1.0 \pm 0.1$	$1.2 \pm 0.1$

a) Reference 30. b) This work.

**Activation Parameters.** The second-order rate constants of  $k_{\text{et}}$  and  $k_{\text{b}}$  at various temperatures (10–30 °C) provide the activation parameters for the quenching and thermal back ET reactions (Tables S1 and S2 in Supporting Information). Figure 4 displays the Eyring's plots produced by the following eq 5:

$$\ln k/T = -\Delta H^\ddagger/T + \Delta S^\ddagger/R + \ln k_{\text{B}}/h \quad (5)$$

Here,  $T$ ,  $R$ ,  $k_{\text{B}}$ , and  $h$  are the absolute temperature, the gas constant, the Boltzmann constant, and Planck's constant, respectively. We estimated the activation enthalpy,  $\Delta H^\ddagger$ , from the slope and the activation entropy,  $\Delta S^\ddagger$ , from the intercept of the linear plots of  $\ln k/T$  versus  $T^{-1}$  that fitted well to the experimental points. For the quenching reaction, the activation parameters  $\Delta H^\ddagger = 17.3 \pm 1.2 \text{ kJ mol}^{-1}$  and  $\Delta S^\ddagger = -49 \pm 3 \text{ J mol}^{-1} \text{ K}^{-1}$  for  $(R,R)$ -[BMV] $^{2+}$  and  $\Delta H^\ddagger = 23.8 \pm 1.7 \text{ kJ mol}^{-1}$  and  $\Delta S^\ddagger = -28 \pm 2 \text{ J mol}^{-1} \text{ K}^{-1}$  for  $(S,S)$ -[BMV] $^{2+}$  were obtained (Table 3). In the case of the thermal back ET reaction,  $\Delta H^\ddagger = 26.5 \pm 1.9 \text{ kJ mol}^{-1}$  and  $\Delta S^\ddagger = -2.4 \pm 0.2 \text{ J mol}^{-1} \text{ K}^{-1}$  for  $(R,R)$ -[BMV] $^{\bullet+}$  and  $\Delta H^\ddagger = 20.3 \pm 1.4 \text{ kJ mol}^{-1}$  and  $\Delta S^\ddagger = -22 \pm 2 \text{ J mol}^{-1} \text{ K}^{-1}$  for  $(S,S)$ -[BMV] $^{\bullet+}$  were also determined from Figure 4.

To evaluate these activation parameters, the energy differences of  $\Delta\Delta H^\ddagger(\text{R-S})$  and  $T\Delta\Delta S^\ddagger(\text{R-S})$  at 25 °C for the quenching and thermal back ET reactions were calculated and are listed in Table 3. Slightly negative  $\Delta\Delta H^\ddagger(\text{R-S}) = -6.5 \pm 1.7$  and  $T\Delta\Delta S^\ddagger(\text{R-S}) = -6.3 \pm 1.0 \text{ kJ mol}^{-1}$  appeared in the quenching reaction, indicating that the stereoselective quenching reaction was dominated by both enthalpy and entropy terms. On the other hand, slightly positive  $\Delta\Delta H^\ddagger(\text{R-S}) = 6.2 \pm 1.9 \text{ kJ mol}^{-1}$  and  $T\Delta\Delta S^\ddagger(\text{R-S}) = 5.8 \pm 1.0 \text{ kJ mol}^{-1}$  ( $\Delta\Delta S^\ddagger = 19 \pm 2 \text{ J mol}^{-1} \text{ K}^{-1}$ ) were obtained at 25 °C in the thermal back ET reaction. Although these  $\Delta\Delta H^\ddagger$  and  $\Delta\Delta S^\ddagger$  values are positive and much different from those of quenching, the difference in the enthalpy change is compensated by the entropy term (Figure 5).<sup>50–52</sup> The stereoselectivity of 1.3 for  $(R,R)$ -[BMV] $^{\bullet+}$  found at low temperature (10 °C) was due to its large  $\Delta S^\ddagger$  value of  $-2.4 \pm 0.2 \text{ J mol}^{-1} \text{ K}^{-1}$  obtained in the thermal back ET reaction. Therefore, a positive  $T\Delta\Delta S^\ddagger$  value discovered in the thermal back ET reaction from [BMV] $^{\bullet+}$  to ZnMb $^{\bullet+}$  surface may be ascribed to the dehydration of the [BMV] $^{\bullet+}$  ion and the amino acid residue on the ZnMb $^{\bullet+}$  surface.<sup>32</sup>

From these experimental results, the differences in the ET stereoselectivities between [BMV] $^{2+}$  and [OAV] $^{2+}$  or [NOAV] $^{2+}$  may mainly arise from their spacial structures. Two chiral centers connected by amide spacer in the [OAV] $^{2+}$

or [NOAV] $^{2+}$  ion have bulky aromatic moieties and these are significant structural factors in efficient stereoselective photo-induced ET reactions with ZnMb. In the case of [BMV] $^{2+}$ , the chiral center is very near the reactive center but lacks the hydrogen bonding of the –CONH– group of the chiral viologen

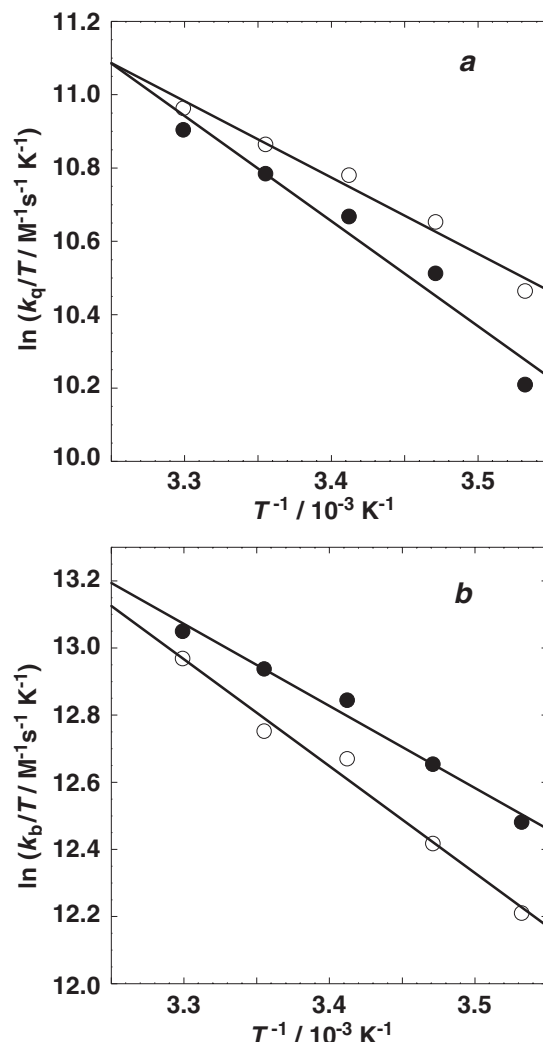


**Figure 4.** Eyring's plots for the quenching and thermal back ET reaction at pH 7.0 (0.010 M phosphate buffer) and  $I = 0.020 \text{ M}$ . (a) Quenching reaction of  $^3(\text{ZnMb})^*$  by  $(R,R)$ -[BMV] $^{2+}$  (open symbols) and  $(S,S)$ -[BMV] $^{2+}$  (closed symbols). (b) Thermal ET reaction of ZnMb $^{\bullet+}$  by  $(R,R)$ -[BMV] $^{\bullet+}$  (open symbols) and  $(S,S)$ -[BMV] $^{\bullet+}$  (closed symbols).

**Table 3.** Activation Parameters for the Quenching Reaction of  $^3(\text{ZnMb})^*$  by  $(R,R)$ -[BMV] $^{2+}$  and  $(S,S)$ -[BMV] $^{2+}$  and the Thermal ET Reaction between ZnMb $^{\bullet+}$  and  $(R,R)$ -[BMV] $^{\bullet+}$  and  $(S,S)$ -[BMV] $^{\bullet+}$  at pH 7.0 (0.010 M Phosphate Buffer) and  $I = 0.020 \text{ M}$

	$\Delta H^\ddagger$ /kJ mol $^{-1}$	$\Delta\Delta H^\ddagger(\text{R-S})$ /kJ mol $^{-1}$	$\Delta S^\ddagger$ /J mol $^{-1} \text{ K}^{-1}$	$\Delta\Delta S^\ddagger(\text{R-S})$ /J mol $^{-1} \text{ K}^{-1}$	$T\Delta\Delta S^\ddagger(\text{R-S})^a$ /kJ mol $^{-1}$
$(R,R)$ -[BMV] $^{2+}$	$17.3 \pm 1.2$	$-6.5 \pm 1.7$	$-49 \pm 3$	$-21 \pm 3$	$-6.3 \pm 1.0$
$(S,S)$ -[BMV] $^{2+}$	$23.8 \pm 1.7$		$-28 \pm 2$		
$(R,R)$ -[BMV] $^{\bullet+}$	$26.5 \pm 1.9$	$6.2 \pm 1.9$	$-2.4 \pm 0.2$	$19 \pm 2$	$5.8 \pm 1.0$
$(S,S)$ -[BMV] $^{\bullet+}$	$20.3 \pm 1.4$		$-22 \pm 2$		

a) Estimated at 25 °C.

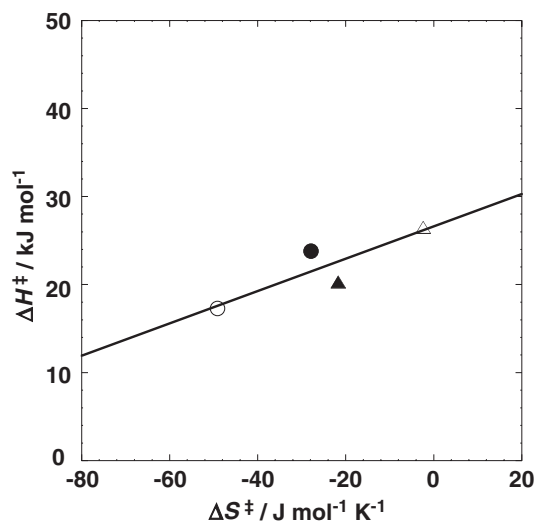


**Figure 5.** Plots of  $\Delta H^\ddagger$  versus  $\Delta S^\ddagger$  values for the ET reactions of ZnMb with  $[\text{BMV}]^{2+}$ : (open circle)  $k_q$  for  $(R,R)\text{-}[\text{BMV}]^{2+}$ ; (closed circle)  $k_q$  for  $(S,S)\text{-}[\text{BMV}]^{2+}$ ; (open triangle)  $k_b$  for  $(R,R)\text{-}[\text{BMV}]^{\bullet+}$ ; (closed triangle)  $k_b$  for  $(S,S)\text{-}[\text{BMV}]^{\bullet+}$ .

with the side chain of the polypeptide of Mb, and the chiral substituent gives small conformational difference between the S,S and R,R isomers. Thus, we finally propose that further modification at the chiral centers of  $[\text{BMV}]^{2+}$  with a bulky substituent should realize remarkably stereoselective photoinduced ET reactions with ZnMb.

### Conclusion

The present study demonstrates stereoselective photoinduced ET reactions between optically active  $[\text{BMV}]^{2+}$  ion and ZnMb. The stereoselectivities both in the quenching and thermal back ET reactions are not large, compared to those of  $[\text{OAV}]^{2+}$  and  $[\text{NOAV}]^{2+}$  systems. These results imply that the bulky aromatic substituent seems to be more important than the distance from the chiral center to the viologen moiety in order to enhance the ET stereoselectivity. We believe that further synthetic applications at the chiral center of  $[\text{BMV}]^{2+}$  based on this insight will produce diverse sets of chiral organic electron carriers. Investigations of fundamental photoinduced ET reactions with hemoproteins may provide valuable information for elucidating the complicated mechanisms of biological stereoselective ET.

This research was partly supported by Grant-in-Aid for Scientific Research No. 19550064 from the Ministry of Education, Culture, Sports, Science and Technology (MEXT) of Japanese Government, Research for Promoting Technological Seeds from Japan Science and Technology Agency (JST) and Nara Women's University Intramural Grant for Project Research. The authors thank Professor Kuninobu Kasuga of Shimane University for elemental analyses.

### Supporting Information

Kinetic, absorption, and CD spectral, and electrochemical data of  $[\text{BMV}]^{2+}$ . This material is available free of charge on the web at <http://www.csj.jp/journals/bcsj/>.

### References

- 1 N. M. Kostić, in *Metal Ions in Biological Systems*, ed. by H. Siegel, A. Siegel, Marcel Dekker, New York, **1991**, Vol. 27, pp. 129–182.
- 2 G. McLendon, R. Hake, *Chem. Rev.* **1992**, 92, 481.
- 3 K. Tsukahara, M. Okada, S. Asami, Y. Nishikawa, N. Sawai, T. Sakurai, *Coord. Chem. Rev.* **1994**, 132, 223.
- 4 D. S. Bendall, *Protein Electron Transfer*, BIOS Scientific Publishers Ltd., Oxford, **1996**.
- 5 J. M. Nocek, J. S. Zhou, S. D. Forest, S. Priyadarshy, D. N. Beratan, J. N. Onuchic, B. M. Hoffman, *Chem. Rev.* **1996**, 96, 2459.
- 6 H. B. Gray, J. R. Winkler, in *Electron Transfer in Chemistry*, ed. by V. Balzani, Wiley-VCH, Weinheim, **2001**, Vol. 3, pp. 3–23.
- 7 H. B. Gray, J. R. Winkler, *Quart. Rev. Biophys.* **2003**, 36, 341.
- 8 H. B. Gray, J. R. Winkler, in *Biological Inorganic Chemistry, Structure and Reactivity*, ed. by I. Bertini, H. B. Gray, E. I. Stiefel, J. S. Valentine, University Science Books, Sausalito, **2007**, pp. 261–277.
- 9 H. Zemel, B. M. Hoffman, *J. Am. Chem. Soc.* **1981**, 103, 1192.
- 10 J. S. Zhou, J. M. Nocek, M. L. DeVan, B. M. Hoffman, *Science* **1995**, 269, 204.
- 11 E. V. Pletneva, D. B. Fulton, T. Kohzuma, N. M. Kostić, *J. Am. Chem. Soc.* **2000**, 122, 1034.
- 12 Z.-X. Liang, J. M. Nocek, I. V. Kurnikov, D. N. Beratan, B. M. Hoffman, *J. Am. Chem. Soc.* **2000**, 122, 3552.
- 13 S. M. Tremain, N. M. Kostić, *Inorg. Chim. Acta* **2000**, 300–302, 733.
- 14 B. M. Hoffman, M. A. Ratner, *J. Am. Chem. Soc.* **1987**, 109, 6237.
- 15 G. McLendon, K. Pardue, P. Bak, *J. Am. Chem. Soc.* **1987**, 109, 7540.
- 16 S. Papp, J. M. Vanderkooi, C. S. Owen, G. R. Holtom, C. M. Philips, *Biophys. J.* **1990**, 58, 177.
- 17 J. Feitelson, G. McLendon, *Biochemistry* **1991**, 30, 5051.
- 18 N. Barboy, J. Feitelson, *Biochemistry* **1987**, 26, 3240.
- 19 N. Barboy, J. Feitelson, *Biochemistry* **1989**, 28, 5450.
- 20 K. Tsukahara, S. Asami, *Chem. Lett.* **1991**, 1337.
- 21 T. Hayashi, T. Takimura, H. Ogoshi, *J. Am. Chem. Soc.* **1995**, 117, 11606.
- 22 T. Hayashi, A. Tomokuni, T. Mizutani, Y. Hisaeda, H. Ogoshi, *Chem. Lett.* **1998**, 1229.
- 23 R. Satoh, Y. Ohba, S. Yamauchi, M. Iwaizumi, C. Kimura, K. Tsukahara, *J. Chem. Soc., Faraday Trans.* **1997**, 93, 537.
- 24 D. A. Geselowitz, H. Taube, *J. Am. Chem. Soc.* **1980**, 102, 4525.
- 25 K. Bernauer, J.-J. Sauvain, *J. Chem. Soc., Chem. Commun.* **1988**, 353.
- 26 J. R. Pladziewicz, M. A. Accola, P. Osvath, A. M. Sargeson, *Inorg. Chem.* **1993**, 32, 2525.
- 27 S. Sakaki, Y. Nishijima, H. Koga, K. Ohkubo, *Inorg. Chem.* **1989**, 28, 4061.
- 28 J. T. Ficke, J. R. Pladziewicz, E. C. Sheu, A. G. Lappin, *Inorg. Chem.* **1991**, 30, 4282.
- 29 K. Bernauer, M. Monzone, P. Schürmann, V. Viette, *Helv. Chim. Acta* **1990**, 73, 346.
- 30 K. Tsukahara, C. Kimura, J. Kaneko, K. Abe, M. Matsui, T. Hara, *Inorg. Chem.* **1997**, 36, 3520.

- 31 K. Tsukahara, R. Ueda, *Bull. Chem. Soc. Jpn.* **2003**, 76, 561.
- 32 H. Takashima, M. Tanaka, Y. Hasegawa, K. Tsukahara, *J. Biol. Inorg. Chem.* **2003**, 8, 499.
- 33 H. Takashima, A. Araki, K. Takemoto, N. Yoshikawa, K. Tsukahara, *J. Biol. Inorg. Chem.* **2006**, 11, 316.
- 34 K. Tsukahara, J. Kaneko, T. Miyaji, K. Abe, M. Matsuoka, T. Hara, T. Tanase, S. Yano, *Bull. Chem. Soc. Jpn.* **1999**, 72, 139.
- 35 K. Tsukahara, R. Ueda, M. Goda, *Bull. Chem. Soc. Jpn.* **2001**, 74, 1303.
- 36 K. Tsukahara, *Inorg. Chim. Acta* **1986**, 124, 199.
- 37 K. Tsukahara, S. Asami, M. Okada, T. Sakurai, *Bull. Chem. Soc. Jpn.* **1994**, 67, 421.
- 38 A. C. Shosheva, P. K. Christova, B. P. Atanasov, *Biochim. Biophys. Acta* **1988**, 957, 202.
- 39 K. Tsukahara, *Trends Inorg. Chem.* **1991**, 2, 17.
- 40 L. A. Dummers, *The Bipyridinium Herbicides*, Academic Press, London, **1980**.
- 41 C. L. Bird, A. T. Kuhn, *Chem. Soc. Rev.* **1981**, 10, 49.
- 42 T. M. Bockman, J. K. Kochi, *J. Org. Chem.* **1990**, 55, 4127.
- 43 S. Aono, S. Nemoto, I. Okura, *Bull. Chem. Soc. Jpn.* **1992**, 65, 591.
- 44 K. Tsukahara, M. Okada, *Chem. Lett.* **1992**, 1543.
- 45 R. A. Marcus, *Discuss. Faraday Soc.* **1960**, 29, 21.
- 46 R. A. Marcus, *J. Phys. Chem.* **1968**, 72, 891.
- 47 J. R. Winkler, H. B. Gray, *Chem. Rev.* **1992**, 92, 369.
- 48 J. A. Cowan, H. B. Gray, *Inorg. Chem.* **1989**, 28, 2074.
- 49 K. Tsukahara, C. Kimura, J. Kaneko, T. Hara, *Chem. Lett.* **1994**, 2377.
- 50 T. K. Harris, V. L. Davidson, *Biochemistry* **1993**, 32, 14145.
- 51 M. R. Mauk, J. C. Ferrer, A. G. Mauk, *Biochemistry* **1994**, 33, 12609.
- 52 G. C. Kresheck, L. B. Vitello, J. E. Erman, *Biochemistry* **1995**, 34, 8398.